Experimental Research of the Influence of Constraint for Pneumatic Artificial Muscle Characteristic

Zang Kejiang, Ma Yan
College of electromechanical engineering
Northeast Forestry University
Harbin, China
kjzang@163.com

Sun Ning, Li Xiuchen, Zhang Lan
College of mechanical engineering
Jiamusi University
Jiamusi, China

***Abstract*—Pneumatic artificial muscle (PAM) is a new pneumatic actuator. A lot of work have been completed about the principle, theoretical, experimental modeling and applications of pneumatic artificial muscle. Researchers have found that PAMs exhibit non-linear characteristic. Base on the published literatures, non-linear characteristic related to elasticity, friction between rubber and braid and the constraint ring. The former two aspects have been mainly studied in the published papers. However, study on the influence of constrains on the end of pneumatic artificial muscle is still rare. This study establishes the PAM static characteristic experimental system, and the PAM characteristics about multiple constraints are tested. Through the analysis of experimental results, the influence is obtained which constraints the work for pneumatic artificial muscle working characteristics.**

***Keywords*—pneumatic artificial muscle (PAM), constraints, static characteristics, experimental research**

I. INTRODUCTION

Pneumatic artificial muscle is a new kind of pneumatic actuator with the advantages of cleanness, lightweight, low cost, easy maintenance, compact structure and high power/volume ratio. For this reason, they are widely concerned by academic study and engineering application. The pneumatic muscle was invented in 1950s in order to provide drivers for prosthesis or rehabilitation mechanical. However, for the practical problems, such as pneumatic power storage, availability and poor quality valve technology at that time, pneumatic artificial muscle have not been developed and applied. In the 1988s, engineers of the Japanese type manufacture Bridgestone proposed more powerful version of the redesigned pneumatic artificial muscle called Rubbertuator intended to motorise though soft yet powerful robot arms. They were called Soft-Arms and were commercialized as service robots which have also been studied. The artificial muscle, which is simple in design, is made of rubber inner tube covered with a shell braided according to helical weaving. The muscle is closed by two ends, one being the air input and the other being force attachment point. The braid fibers run helically about the muscle's long axis at an angle called interweave angle. When pressure is supplied, the inner tube transformed, together with sets of radial movement driving weaving, interweave angle increasing, the axial braid sleeve shorting which pulling the end of the load and weaving sets of filaments produced tension at the same time, then the tension and internal pressure equilibrium. Because of PAM's working characteristics similar to animal muscle, it is called pneumatic actuator pneumatic artificial muscle [1] [2]. Pneumatic artificial muscle is a new pneumatic actuator. A lot of work have been completed about the principle, theoretical, experimental modeling and applications of pneumatic artificial muscle. Researchers have found that PAMs exhibit non-linear characteristic. Base on the published literatures[3] [4], non-linear characteristic related to elasticity, friction between rubber and braid and the end constraints. The former two aspects have been mainly studied in the published papers. However, study on the influence of the constraints on the end of pneumatic artificial muscle is still rare. This study establishes the PAM static characteristic experimental system, and the PAM characteristics about multiple constraints are tested. Through the analysis of experimental results, the influence that constraints work for pneumatic artificial muscle working characteristic is obtained.

II. EXPERIMENTAL PNEUMATIC SYSTEM

A. Experimental rig

This pneumatic experimental system （Fig.1） is designed to study the relationships of the pressure, contraction and force of PAMs with different constraints. The experimental system contains elements shown in the following table.

TABLE I. DETAIL SHEET

Component name	Component type	Component technical data
air source	Fuma-CEBM	power:11KW maximum pressure: 0.8MPa gasholder: 2L
solenoid valves	FESTO-R107	supply voltage : DC24V out press：0-0.6MPa
pressure sensor	SMC PSE540A-R06	supply voltage : DC 12 ~ 24V pressure range:0-1MPa accuracy: ± 0 • 5%
load sensor	CZL-3	supply voltage : DC 12 ~ 24V load range: 0-50Kg accuracy: ± 0 • 03%
PAM	Home-made	initial length: 176mm initial diameter: 8mm

978-1-4244-8452-2/11/$26.00 ©2011 IEEE

		pressure range:0-0.3 MPa
stepper motor	86BYGH450B-113	step angle accuracy:2% step angle:1.8° max torque：6.7Nm
guide screw	SFU1605	nominal diameter：16mm lead:5mm rated load:7.65KN
displacement sensor	KTC 500	lin: ± 0.058 R: 5.3KΩ
computer	LEGEND 1+1	CPU: Pentium III 450 RAM : 256M
data collector	WS-USB	resolution: 8 accuracy:0.003%FS ± 1LSB
driver	CW250AC	supply Voltage : DC12~24V mode of operation: 1/5、1/10 、1/25 、1/40 、1/50 、1/100 、1/200
pulser	MPTG	supply Voltage :DC100~250V output Frequency : 6-9999Hz
weight	components of national standards	2Kg
reducing valve	IR2020-02G-R	max sup press: 1MPa out press: 0.01-0.8MPa

Figure 1. Pneumatic experimental system

The feed equipment is composed of four parts : stepper motor, pulser, driver and guide. The pulser outputs pulses to stepper motors drivers to drive the stepper motors forward or backward. The pulser can be measured in 1/4998. The stepper motor turns a full circle by 200-steps. The lead of screw is 5mm/r. The position error is little (about 5e-6mm/r). Straight line lead rails are adopted in the experimental system, with good accuracy and stabilization.

Fig.1 shows an ordinary pneumatic experimental system. The computer-controlled solenoid valves can output a predetermined gas pressure. When compressed gas enters PAM, it contracts and produces a pulling force. The gas source is usually a compressor. Clearly the experiment should include both a solenoid valves and PAM. First we discuss the solenoid valves. This is a computer-controlled system outputs a predetermined gas pressure within a definite field which is proportional to the voltage which as a solenoid valves' input, whose quantity can be controlled by the computer.

The pneumatic experimental system consists of a pressure sensor, a load sensor and a displacement sensor. The pressure sensor measures the output gas pressure, the load sensor measures the output load, and feed these back to the control circuit. The magnitude of the gas pressure output from the compressor should be larger than the maximal gas pressure output from the solenoid valves.

B. Muscle

The artificial muscle consists of the inner rubber tube where the natural rubber latex through the vulcanizing process has been used as shown in Fig.2. In order to reduce the influence of the rubber elastic, the rubber used in the experimental is very thin. The outer shell is the braided sleeve (see Fig.2).

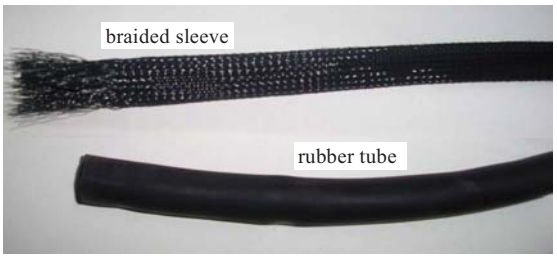

Figure 2. Rubber tube and braided sleeve

The assembly of the artificial muscle is shown in Fig.3, one side of which is the air inlet and the other side is the closed end. In this experiment, four types of the number of the constraint rings (0, 1, 2, 4) have been tested [5].

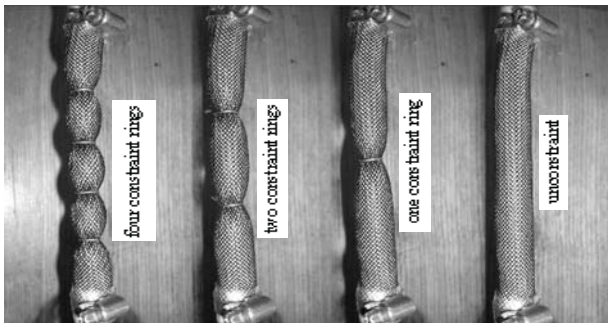

Figure 3. Pneumatic artificial muscle with constraint rings

III. ISOMETRIC-LOAD EXPERIMENT

The experiment setup is shown in Fig.4. One end of PAM 5 is mounted tightly to a metal frame. The other end of the muscle is tied by wire rope with different loads suspended to it. Displacement sensor 8 is fixed to the metal frame; slide rod is connected to removable end of the muscle, so that a precise measurement is made. The position data obtained from displacement sensor is sent back to the PC through the A/D converter. To provide the power for the muscle, air compressor 1 can supply 0.8MPa compressed air. The computer-controlled solenoid valves 2 can output a predetermined gas pressure. In this test, weights 7 are 4Kg and 6Kg. Compressed gas enters muscle, PAM contracts while the weight is able to maintain constant pulling force. The real-time data through the sensors are logged to the PC. The experiment is repeated several times under different constraints. Then we can statistically analyze

the results to find out the relationship between the contraction ratio and pressure of the muscle for different load [6] [7] [8] [9].

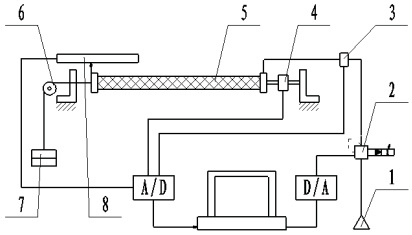

Figure 4. Principle block diagram of isometric-load experimental system

The length of muscle is measured by displacement sensor, l_0 is initial length, l is real-time length, then contraction ratio ε is calculated as

$$\varepsilon = (l_0 - l)/l_0 \tag{1}$$

Fig.5 shows the relation between contraction ratio and pressure. From this figure, we can obviously conclude that the experimental curve is a hysteresis curve, this is because of a change in direction of friction when the PAM working during a test period. And at low pressure, the experimental curve shows more hysteresis than at high pressure. This kind of phenomenon is referred to the internal friction coefficient of PAM and filling pressure [10].

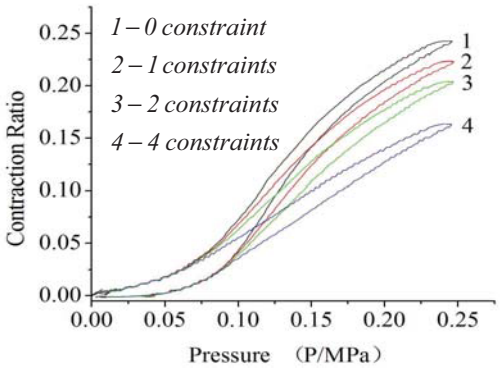

Figure 5. Pressure versus contraction ratio

In order to highlight the influence of constraints, constraint ring diameter slightly larger than the initial diameter of PAM. When the contraction ratio reaches a certain value, the constraint rings begin to work on the PAM. When constraint rings don't work, the experiment curves are superposition; when constraint rings under working, the contraction is obviously smaller when increasing the constraint rings in the same pressure. Constraints reduce the PAM contraction ability.

IV. ISOMETRIC- PRESSURE EXPERIMENT

Isometric-pressure experiment studies the relationship between the contraction ratio and force under certain constant pressure. One end of PAM 5 is mounted tightly to a metal frame through load sensor 4. The other end of the muscle is attached on a slide plate sliding along linear guides, and the slide plate employs guide screw 7 controlled by a stepper motor 6, these transmission components are able to simultaneously obtain high control accuracy and operating efficiency. In this test, Pressure valve set pressure at 0.1MPa, 0.15MPa, 0.2Mpa and 0.25MPa. Then by using the motor to change the length of the muscle under the corresponding pressures mentioned above. The data of pulling force and displacement through the sensors （4,6） are sent to the PC. The experiment is repeated several times under different constraints. We can carry out different constraint isometric-pressure experiments under the different pressure [11].

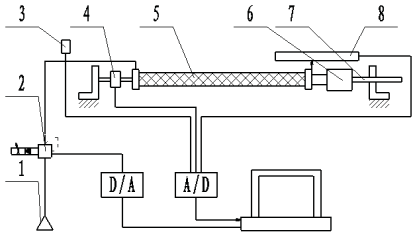

Figure 6. Principle block diagram of Isometric- pressure experimental system

Fig.7 shows the relation between contraction ratio and force. The output force of PAM is related to contraction ratio, the greater the contraction ratio, the greater the output force. As mentioned above, the PAM isometric-pressure curve is a hysteresis curve due to the influence of friction. With the increase in the number of constraints, there exists significant hysteresis phenomenon, the experimental curves drop as a whole, the linearity degree become poor, but the trend do not change, which clearly indicate that constraints are significantly impacts the static characteristics of PAM.

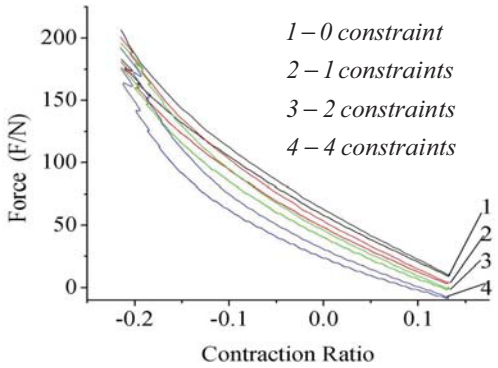

Figure 7. Contraction ratio versus force

V. ISOMETRIC-LENGTH EXPERIMENT

The experiment rig is shown in Fig.8. One end of PAM 5 is fixed on frame. The other end of the muscle connects a slide plate sliding along linear guides which is the same structure as Isometric-pressure experiment system. The system is composed of a slide plate, a guide screw 7 and a stepper motor 6 self-lock device which is used to accurately change the length of muscle. The computer-controlled solenoid valves 2 can make gas pressure change regularly. When compressed gas enters the muscle, a pulling force is produced and working on the load sensor 4. The load data obtained from load sensor is sent back to the PC through the A/D converter. The guide screw is caused to rotate by means of stepper motor to change length of the muscle. The experiment is repeated several times using different constraints (0, 1, 2, 4).

Fig.9 shows the relation between pressure and force. The result is a load cycle of actuator force in the range of operational pressure. Fig.9 shows that force decreases with actuator constraint. Tiny force is almost always measured during the decreasing pressure phase of the test [12].

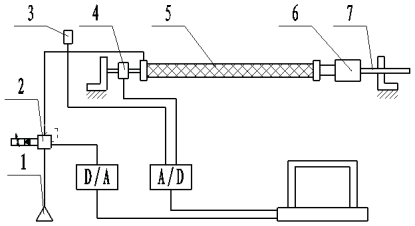

Figure 8. Principle block diagram of isometric-length experimental system

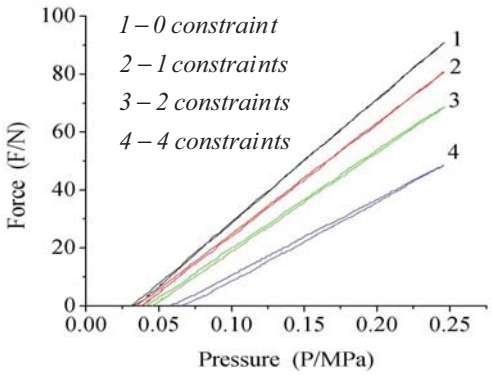

Figure 9. Pressure versus force

Fig.9 also shows that the output force of pneumatic artificial muscle is proportional to inflation pressure. However, during this test, friction between rubber tube and braided sleeve is very small; the hysteretic behavior appears to decrease. The rubber thickness, which is used in this experimental, is small. The rubber elastic force is small. The graph clearly shows that the system mentioned above have a little influence to this experiment. The linear relationship between pressure and output force do not change when the number of constraints increasing. However, there is a change in their slope. Without the influence of the rubber elastic force and friction between rubber tube and braided sleeve, the constraint influence is obvious.

VI. COMPARISON OF MODEL TO EXPERIMENT

In order to verify whether the results are reasonable, a theoretical approach is introduced without considering the detailed geometric structure modified from the work reported in.

To find the equation of the muscle force by using the principle of virtual work, there must be an equilibrium between the virtual work dW_{in} done in the muscle by the pressure and the virtual work done by the displacement of the muscle dW_{out} [11] (see Fig.10).

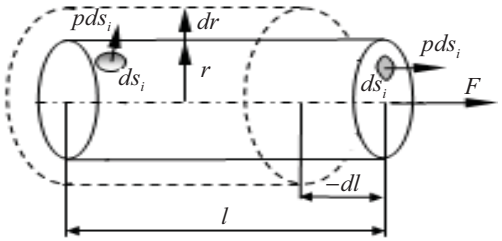

Figure 10. Schematic diagram of the two interacting virtual work components.

dW_{in} can be calculated with the help of the relative pressure p, the surface of the pressure attack S_i, the normal vector on ds_i, the working direction of the resulting force dl_i and the change of the muscle volume dV:

$$\begin{aligned} dW_{in} &= \int_{S_i} p \cdot ds_i \cdot dl_i \\ &= p \cdot \int_{S_i} ds_i \cdot dl_i \\ &= pdV \end{aligned} \tag{2}$$

The axial force F and the muscle axial displacement dl produce the outer virtual work

$$dW_{out} = -F \cdot dl \tag{3}$$

By equating both the virtual work components and using (2) and (3), the equation for the muscle force is derived.

$$dW_{in} = dW_{out} \tag{4}$$

$$F = -P \cdot \frac{dV}{dl} \tag{5}$$

By assuming that the contracting muscle surface acts the similar as a cylinder, dW_{in} can be divided into an axial and a radial components. The axial component has the opposite working direction to the radial component, see Fig.10. The force equation is found:

$$F = 2\pi rrlp\frac{dr}{dl} - \pi r^2 p \tag{6}$$

A PAM is modeled as a cylinder and the wall thickness is assumed to be zero. The dimensions of this cylinder are the length l and diameter $D = 2r$. Assuming inextensibility of the mesh material, the geometric constants of the system are the thread length b and the number of turns for a single thread n. The final dimension used for this formulation is the interweave angle θ, which is the angle between the thread and the long axis of the cylinder. The interweave angle changes as the length of the actuator changes. The relationship between these parameters is shown in Fig. 11[13].

With the help of Fig. 11 the correlation between muscle radius r, muscle length l and interweave angle θ formulated. Due to the fact, that the length of the fibers is constant one finds that $\frac{l}{l_0} = \frac{\cos\theta}{\cos\theta_0}$ and $\frac{r}{r_0} = \frac{\sin\theta}{\sin\theta_0}$. l_0 is the initial length, r_0 is the initial radius, θ_0 is the initial interweave angle. This is used to calculate the correlation between r and l:

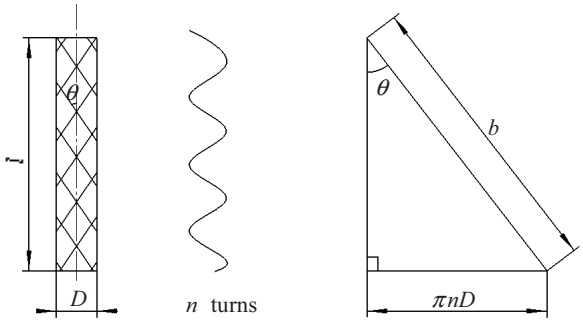

Figure 11. Geometric model of PAM

$$r = r_0 \frac{\sqrt{1-\cos^2\theta_0}}{\sin\theta_0} = r_0 \frac{\sqrt{1-\left(\cos\theta_0 \cdot \frac{l}{l_0}\right)^2}}{\sin\theta_0} \tag{7}$$

hence

$$\frac{dr}{dl} = -\frac{r_0 l \cos^2\theta_0}{l_0^2 \sin\theta_0} \cdot \frac{1}{\sqrt{1-\left(\cos\theta_0 \frac{l}{l_0}\right)^2}} \tag{8}$$

By using (6), (7) and (8), the force can be calculated:

$$F = \pi r_0^2 p\left(\frac{3}{\tan^2\theta_0} \cdot \frac{l^2}{l_0^2} - \frac{1}{\sin^2\theta_0}\right) \tag{9}$$

The correlation of force F, pressure p and contraction $\varepsilon = (l_0 - l)/l_0$, due to diameter D_0 is directly measured $D_0 = 2r_0$.

$$F = P\left[\frac{3\pi D_0^2}{4\tan^2\theta_0}(1-\varepsilon)^2 - \frac{\pi D_0^2}{4\sin^2\theta_0}\right] \tag{10}$$

The formulation described in this section follows the work of Chou and Hannaford in modeling PAM [2]. Next, these equations will be used to derive further relationships among force, pressure, length. These relationships will then be verified and fine-tuned with empirical data.

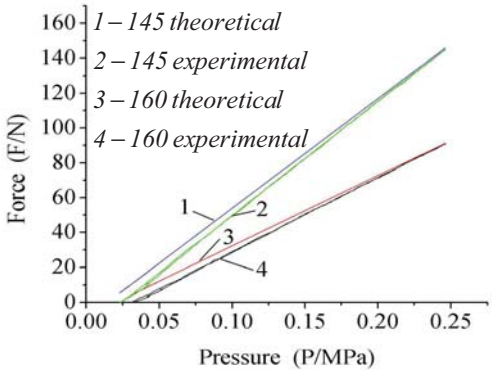

Figure 12. Pressure versus force

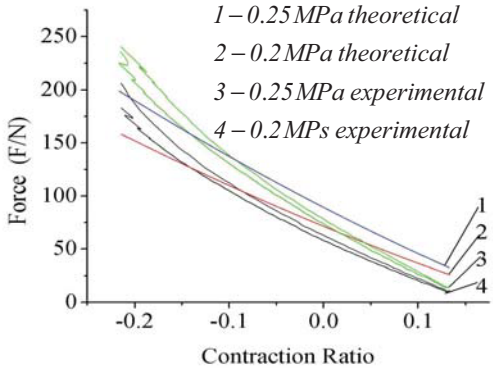

Figure 13. Contraction ratio versus force

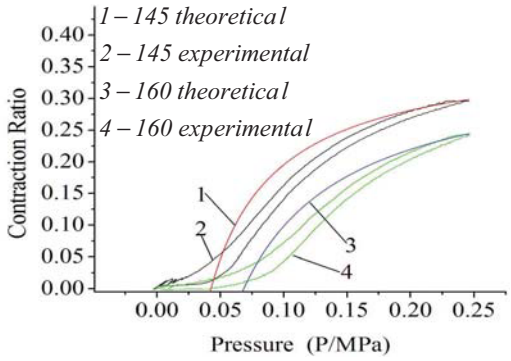

Figure 14. Pressure versus contraction ratio

VII. CONCLUSION

This paper establishes the PAM static characteristics experimental system for studying constraint influence. By using a self-made pneumatic artificial muscle which employing thin rubber tuber in this experiment, the elastic force of rubber is reduced. Through the comparison of the theoretical model and the experimental curves the reliability of the experiment is proved. Constraint reduces the PAM output force and the contraction. Relative to the working principle, constraints lower the ability of contract and limit PAM inflation. However, theoretical formula of the result has not been derived out so far, there is much work to be done in the future.

ACKNOWLEDGMENT

The authors gratefully acknowledge the support of Heilongjiang Province office of Education science and technology projects (11531372) and Jiamusi University science and technology project (Lz2011-015) .

REFERENCES

[1] Zang Kejing, Gu Lizhi, Tao Guoliang, “Study and prospect of pneumatic artificial muscle”, Machine Tool & Hydraulics, 2004(4) pp.4-7.

[2] Chou C P, Hannafonl B, “Static and dynamic characteristics of McKibben pneumatic artificial muscles”, In IEEE Conference on Robotics and Automation [C].San Diego,USA: 1994 264-269.

[3] Tian Sheping, Lin Lianming, “Artificial muscle and static characteristic and measurement”, Practical Measurement Technology, 1998(6) pp.12-14.

[4] Huang Yu, Peng Guangzheng, Fan Wei, “Experiment Study of Actuating Characteristics of Pneumatic Artificial Muscle”, Chinese Hydraulics & Pneumatics, 2002(12) pp.9-11.

[5] Sathaporn Laksanacharoen, "Artificial Muscle Construction Using Natural Rubber Latex in Thailand", The 3rd Thailand and Material Science and Technology Conference, Miracle Grand Hotel, Bangkok, Thailand, August 10-11, 2004.

[6] Yang Gang, Li Baoren, Liu Jun, “The new way of pneumatic artificial muscle characteristic analytic”, Hydraulic Pressure and Pneumatic, 2002(10)pp.22-25.

[7] Sun Liming, Bao Gang, Wang Zuwen, “The improve modeling of pneumatic artificial muscle”, Hydraulics Pnerumatics & Seals, 2002(2) pp.1-4.

[8] Du Jingming, Zhu Duanyang, Yang Gang, Li Baoren, “Experimental reserch on the static characteristic of pneumatic muscle actuator”, Chinese Hydraulics & Pneumatics,2005(5)pp. 21-23.

[9] Li Xingfei, Zheng Qi, Zhang Guoxiong, “Mathematic model and experimental study of humanoid peneumatic muscle”. Journal of Tianjin University, 2005(3) pp.242-247.

[10] Nicholas T. Yerkes, Norman M. Wereley, “Pneumatic artificial muscle activation for trailing edge flaps”, 46th AIAA Aerospace Sciences Meeting and Exhibit,2008.pp.7-10.

[11] Masanori Sugisaka, Huailin Zhao, “The characteristics of McKibben muscle based on the pneumatic experiment system”, Artificial Life & Robotics, vol 11,2007.pp.223-226.

[12] Kenneth, K.K.Ku, Robin Bradbeer, “Static model of the shadow muscle under pneumatic testing”, The 4th regional inter-university postgraduate electrical and electronics engineering conference,2006.

[13] T. Kerscher, J. Albiez, J.M. Z¨ollner, R. Dillmann, “Flumut – dynamic modelling of fluidic muscles using quick-release”, 3rd International Symposium on Adaptive Motion in Animals and Mchines,2005.